Published in final edited form as:
J Memb Sci. 2011 November 1; 383(1-2): 44–49. doi:10.1016/j.memsci.2011.08.032.

Effect of β-sheet crystalline content on mass transfer in silk films

Kiran A. Karve[a], **Eun Seok Gil**[b], **Stephen P. McCarthy**[c], and **David L. Kaplan**[b,*]

[a]Biomedical Engineering and Biotechnology Program, University of Massachusetts at Lowell, Lowell MA 01854 USA

[b]Departments of Biomedical Engineering, Chemical and Biological Engineering, Tufts University, 4 Colby Street, Medford MA 02155 USA

[c]Department of Plastics Engineering University of Massachusetts at Lowell, 1 University Avenue, Lowell MA 01854 USA

Abstract

The material properties of silk are favorable for drug delivery due to the ability to control material structure and morphology under ambient, aqueous processing conditions. Mass transport of compounds with varying physical-chemical characteristics was studied in silk fibroin films with control of β-sheet crystalline content. Two compounds, vitamin B12 and fluorescein isothiocynate (FITC) labeled lysozyme were studied in a diffusion apparatus to determine transport through silk films. The films exhibited size exclusion phenomenon with permeability coefficients with contrasting trends with increases in β-sheet crystallinity. The size exclusion phenomenon observed with the two model compounds was characterized by contrasting trends in permeability coefficients of the films as a function of β-sheet crystallinity. The diffusivity of the compounds was examined in the context of free volume theory. Apart from the β-sheet crystallinity, size of the compound and its interactions with silk influenced mass transfer. Diffusivity of vitamin B12 was modeled to define a power law relationship with β-sheet crystallinity. The results of the study demonstrate that diffusion of therapeutic agents though silk fibroin films can be directed to match a desired rate by modulating secondary structure of the silk proteins.

Keywords

Silk; *β*-sheet; Diffusion; Permeability; Controlled drug delivery

1. Introduction

Controlled release is desirable for therapeutics as it enables sustained release of drugs within effective therapeutic limits over extended periods of time [1,2]. This control enhances the efficacy of therapeutic agents [1,2]. Synthetic biodegradable polymers such as polyesters [3] and polyanhydrides [4] have been crafted into matrices with well-defined release kinetics. However, limits to the compatibility between the degradation products of these polymers

*Corresponding author: Tel.: +1 617 627 3251; fax +1 617 627 3231. david.kaplan@tufts.edu (D.L. Kaplan).

with the encapsulated therapeutic [2,5] and the surrounding tissue [6,7], limit applications. Natural polymers such as chitosan [8] and collagen [9] have enabled the design of release matrices with biocompatibility and biodegradability, however often modifications [10] or crosslinking [9] are required. Such changes can be problematic in terms of compatibility with the entrapped drug and control of degradation lifetime. Moreover, these polymers are unstable under many processing conditions, such as temperature, pH and other variables [9]. Therefore, there remains a need for biomaterials which (i) excel in biocompatibility and controlled biodegradability, (ii) permit ambient processing conditions and (iii) facilitate efficacious and predictable delivery of a multitude of therapeutic agents.

Over the last decade, silk fibroin obtained from cocoons of *Bombxy mori* (*B. mori*) silkworms has been studied for drug delivery applications. Known typically for high mechanical strength [11], silk is biocompatible [12,13] and biodegradable with control of lifetime from hours to years depending on processing conditions and treatment [14,15]. This tunable characteristic is particularly suited for applications of silk biomaterials for controlled release devices. Furthermore, the properties of silk biomaterials can be manipulated without incorporating harmful chemical agents, thereby positively influencing the utility of silk-based devices for medically-related applications.. Since beta sheet content reflects degradation lifetime in vivo, options for long term implants that retain degradability are also a plus with silk-based devices. The protein can be processed into multiple material formats for encapsulating therapeutic agents. The mild conditions during processing favor the stability of both the therapeutic and the matrix [16–18]. Hence, a number of strategies based on silk coating thickness and β-sheet crystalline content have been used to facilitate controlled release [19–22]. Efforts to understand mass transport in silk biomaterials are limited, and studies into this process can help provide improved fundamental insight as well as more predictable control of drug delivery from silk.

In the present study, the mass transport of model two compounds vitamin B12 and lysozyme was studied as a function of β-sheet crystallinity of silk. Thin films were cast to mimic single layer silk coatings to control drug availability. The β-sheet crystallinity was varied by water annealing (W.A.) and/or methanol annealing (M.A.) during film processing. Mass transfer was analyzed using free volume theory.

2. Materials and Methods

2.1. Materials

Bombyx mori (silkworm) cocoons were supplied by Tajima Shoji Co (Yokohama, Japan). All chemicals, analytical or pharmaceutical grade, were purchased from Sigma-Aldrich (St. Louis, MO, USA) and used as received.

2.2. Preparation of silk films

Aqueous silk fibroin solution was prepared as described previously [23]. Briefly, *B. mori* cocoons were boiled for 30 min in 0.02 M Na_2CO_3 solution to extract the fibroin from the sericin glue-like proteins. The fibers were then dissolved in a 9.3 M solution of lithium bromide at 60°C and dialyzed in Slide-a-Lyser cassettes (MWCO 3500 g/mol) (Pierce, Woburn, MA, USA) against Milli-Q water. The resulting solution was centrifuged to remove any suspended impurities. The concentration of the stock was estimated by weighing the residual solid content of a known volume of fibroin solution. The concentration of the silk fibroin solution was adjusted to 1% (*w/v*) and a 386 μL aliquot, estimated from the relation between fibroin concentration and film thickness [24], was cast on circular poly(dimethoxysiloxane) molds (28 mm diameter) to obtain films with 2 μm thickness. The cast films were dried overnight in a clean chemical hood. β-sheet crystallinity was induced

in the films by four different treatments (i) 6 h W.A., (ii) 15 h W.A., (iii) 15 h W.A. followed by 2 h M.A. or (iv) 2 h M.A. treatments. Films were water annealed by subjecting them to a water vapor environment inside an air evacuated desiccator, partially filled with water for a duration defined by the treatment [24]. To methanol anneal, the films were soaked in a solution of 80% methanol and subsequently rinsed with Milli-Q water to remove traces of solvent.

2.3 Characterization

***2.3.1* Thickness of dry films—**The thickness of the cast films was measured by imaging their cross-sections under a scanning electron microscope. The 2 h M.A. films were freeze fractured in liquid nitrogen and sputter coated with platinum-palladium alloy. The cross-sections were imaged using a Zeiss Ultra 55 Field Emission Scanning Electron Microscope (FESEM) (Carl Zeiss SMT Inc., Germany). Film thicknesses were evaluated using Image J analysis software at three random locations along the cross section. The thickness of the dry film was reported as the average of three films.

2.3.2 Hydration of silk films—The hydration of silk films was studied gravimetrically with films 100 μm thick and 15 mm in diameter. A linear relationship independent of the annealing process was assumed between the thickness of the film and its hydration. Briefly, an annealed film was soaked in Milli-Q water. At regular time intervals, the film was removed from the water, and gently blotted to remove excess water on the surface. The film was weighed and then allowed to soak further in water. The process was repeated until no increase in the weight of the wet films (W_w) (mg) was observed. The films were then dried in an oven and weighed (W_d) (mg). The percent hydration of the film was calculated by (Eq. 1) [25]

$$\%\text{Hydration} = \frac{W_w - W_d}{W_w} \times 100 \quad (1)$$

The percent hydration was reported as an average of five samples for each annealing process.

***2.3.3* Fourier transform infrared spectroscopy (FTIR)—**The changes in the secondary structure of silk resulting from the different annealing treatments were analyzed with a JASCO FT/IR 6200 spectrometer (JASCO, Tokyo, Japan) [26]. The films were scanned 32 times over a wave-number range of 400 – 4000 cm^{-1} with a resolution of 4 cm^{-1}. The spectra were deconvoluted using Opus 5.0 software [27]. The secondary structures of the films were evaluated in the amide I region (1595 – 1705 cm^{-1}) [27]. The β-sheet crystalline content of the films was quantified by integrating the area under the silk II peaks (1614 – 1635 cm^{-1} and 1695 – 1705 cm^{-1}) [27] and normalizing to the total area under the curve in the amide I region.

2.4 Model compounds

Two compounds varying in molecular weight, hydrodynamic radius and ionic character (Table 1) were used to elucidate mass transport across the silk films. Stock solutions of the two compounds vitamin B12 (1mg mL^{-1}) and FITC-lysozyme (0.5 mg mL^{-1}) were prepared in Dulbecco's phosphate buffered saline (DPBS, pH 7.4) and stored at 8°C. Compound standards in DPBS were analyzed with a UV spectrophotometer (Molecular Devices, CA) by measuring the absorbance (λ = 361 nm) for vitamin B12 and florescence ($\lambda_{excitation}$ = 488 nm and $\lambda_{emission}$ = 520 nm) for FITC-lysozyme. Standard curves were

plotted for both compounds. Stability of the compounds for the experiments was ascertained by spectrophotometric analysis of the compound standards incubated at 37°C (data not included).

2.4.1 **Conjugation of fluorescein isothiocynate (FITC) to lysozyme—**FITC labeled lysozyme was synthesized by adding 500 μL of 1 $mg.mL^{-1}$ FITC/dimethyl sulfoxide to a 2 $mg.mL^{-1}$ solution of the protein in 0.1 M carbonate-bicarbonate buffer at pH 9. The reaction was stirred in dark for 12 h and dialyzed against Milli-Q water to remove the salts. The labeled protein was then lyophilized and stored for further use. The fluorescein to protein molar ratio was calculated to be 0.55 as per the manufacturer's instructions. Since the calculated molecular weight of 14.3 kDa of the FITC labeled lysozyme did not vary significantly from that of the unlabeled protein (Table 1), it was assumed to have a negligible effect on the hydrodynamic radius of lysozyme. From the following section, lysozyme and FITC lysozyme have been used inter-changeably in the text.

2.5 Permeation studies

Transport of the model compounds across the silk films with varying crystallinity was studied using a standard horizontal twin cell side-by-side diffusion apparatus (Permegear Inc. Hellertown, PA). The total capacity of each cell in the apparatus was 7 mL. Films equilibrated in DPBS were mounted between the two cells of the apparatus providing a total area of 1.54 cm^2 for diffusion of compounds. Due to the potential for fracture during storage and handling, the silk films were evaluated immediately after the annealing treatments. The compound stock was loaded in the donor cell. An equal volume of DPBS was loaded in the receptor cell. To prevent concentration polarization, solutions in both the cells were stirred with magnetic stir bars at 600 rpm. The temperature was maintained at 37°C with a constant temperature circulating water bath. One hundred μL samples were withdrawn from the receptor cell at defined time points and replaced with equal amounts of DPBS. The samples were analyzed by UV spectrophotometry and concentrations evaluated from standard curves. Background absorbance and auto-fluorescence associated with silk, were accounted for by conducting the experiment without any compounds and subtracting the blank readings from the sample readings at the respective time points.

2.5.1 **Data Analysis—**To calculate the transport parameters, the cumulative mass of a compound permeating through the film was calculated and normalized by the area available for diffusion. These data were then plotted as a function of time. The net flux J, ($mg\ cm^{-2}\ s^{-1}$) of the compound passing through the film was given by the slope of the linear portion this curve ($R^2 > 0.97$). Thus, the permeability coefficients of the silk films were calculated under steady state conditions by Fick's first law of diffusion expressed as (Eq. 2) [28]

$$J = C_0 * P \tag{2}$$

Here, P ($cm\ s^{-1}$) is the permeability coefficient of the film and C_0 ($mg\ mL^{-1}$) is the concentration of the donor chamber maintained at sink conditions. The diffusion coefficients of the model compounds under steady state conditions were calculated from the permeability coefficient using (Eq. 3)

$$D = \frac{P * h}{K_d} \tag{3}$$

Here, D ($cm^2\ s^{-1}$) is the diffusion coefficient, K_d (dimensionless) is the partition coefficient of the model compound between silk and the buffer and h (cm) is the hydrated film thickness. The hydrated film thickness was estimated indirectly, by calculating the swelling ratio of solvent equilibrated 100 μm films.

2.6 Determination of partition coefficient (K_d)

The partition coefficient is a measure of solubility and defines the distribution of the compound in the film relative to that in the surrounding solvent. Higher solubility of the compound in the films is attributed to greater partitioning resulting from strong interactions between the two. For $K_d \leq 1$ the compound is practically insoluble in the film. Partition coefficients of the model compounds between the film and the solvent were estimated using the solvent depletion method. Silk films, 2 μm in thickness and 15 mm in diameter, were soaked in stock solutions of the compounds and allowed to equilibrate. The equilibrium concentrations of the solutions were measured by UV-spectroscopy and partition coefficient was given by (Eq. 4)

$$K_d = \frac{V_s(C_i - C_s)}{V_f C_s} \tag{4}$$

Here, C_i ($mg\ mL^{-1}$) is the initial concentration of compound solution, C_s ($mg\ mL^{-1}$) is the equilibrium drug concentration of the solution, V_s (mL) is the volume of the compound solution, and V_f (cm^3) is the volume of the solvent equilibrated silk films. V_f was calculated using the equivalent hydrated film thicknesses estimated from the swelling ratios of films 100 μm thick. The partition coefficient is reported as an average of three samples for each annealing condition.

2.7 Statistical Analysis

The data were analyzed by single factor analysis of variance (ANOVA). Data were considered statistically significant for $p < 0.05$.

3 Results and Discussion

Silk matrices have been investigated for delivery of a variety of therapeutics such as adenosine, theophylline emodin, bone morphogenic protein (BMP-2) and plasmid DNA [29]. To characterize the transport of this wide range of compounds we have selected vitamin B12 to model small molecule therapeutics and lysozyme for peptide therapeutics.

The function of silk films was investigated for controlled release applications by modifying their β-sheet crystalline content and quantifying mass transport. The β-sheet content of the 2.27 ± 0.14 μm thick films was varied using four different annealing treatments and characterized by FITR spectroscopy. Figure 1 shows the FTIR spectra of the silk films in the amide I (1705 – 1595 cm^{-1}) and amide II (1595 – 1495 cm^{-1}) regions [27]. Also shown is the absorbance spectrum of an as-cast film included as a control. This film exhibited a strong absorbance at 1644 cm^{-1}, characteristic of random coil conformation (Figure 1a) [27]. Water annealing the films resulted in formation of peaks at 1650 cm^{-1} and 1625 cm^{-1}, characteristic of silk I and silk II/β-sheet structures, respectively (Figures 1b, 1c). With methanol annealing, stronger absorbance peaks were observed at 1625 cm^{-1} (silk II/*β*-sheet) while less prominent peaks formed at 1650 cm^{-1} (silk I) (Figures 1d, 1e). The relative ratio of β-sheets was estimated by deconvoluting the spectra and quantifying the area under the peaks. The β-sheet content estimated for 6 h W.A. and 2 h M.A. films (Table 2) were lower

than those observed by Lu *et. al* (6 h W.A. 30.3 ± 0.7%, 1 h M.A. 40.8 ± 2.1%), but followed the same trend with respect to the two treatments [30]. Increasing the duration of water annealing process and treating these films with methanol caused only a minor increase in β-sheets. Further, the increase in β-sheet of the 15 h W.A + 2 h M.A. films may be associated with the inability of silk I formed after water annealing to convert to silk II (β-sheets) on further exposure to methanol [31]. Overall, methanol annealing yielded higher β-sheet content when compared to the water annealing treatments.

3.1 Permeability coefficient

The silk films were studied for permeability with two different compounds that varied in molecular weight, hydrodynamic radius and ionic character (Table 1) using a twin cell apparatus. Figure 2 shows the change in the receptor cell concentration as a function of time for vitamin B12 diffusing across films annealed by the four different processes. The permeability coefficients of the films were calculated using equation 2 and are listed in Table 2. Compared to lysozyme, the films were more permeable to vitamin B12, presumably due to its smaller hydrodynamic radius and non-ionic character. Moderation in the crystalline content of the films did not affect this size exclusion phenomenon. However, an increase in the crystalline content of the films yielded contrasting permeability profiles with the two compounds.

Overall, for vitamin B12, the permeability of the silk films decreased with increase in β-sheet crystalline content. This may be attributed to the reduction in hydration of the films with increase in β-sheets (Figure 3). The β-sheets can be considered as physical cross-links, which restrict swelling of the films in a buffer. Hence, the presence of increased β-sheets decreased the solvent phase available in the films to diffuse vitamin B12, thereby decreasing the permeability. Although, partitioning of vitamin B12 was observed between the silk films and the buffer, this did not influence the observed permeability trend (Table 2). The smaller size of the molecule likely played a role in minimizing the impact of these interactions. Overall, the partitioning of vitamin B12 increased with increase in β-sheet content. However, this was significantly greater only with the 2 h M.A. films and may have contributed synergistically with the low hydration of these films towards the observed permeability. The only contradiction to the observed trend between β-sheet content and permeability was for the 15 h W.A. films. The increase in the permeability of these films did not follow the rationale based on film hydration and compound partitioning. This result suggested that permeability of the films could involve other complex factors that were not discernable within the limits of the present study.

Interestingly, the permeability of the silk films increased for lysozyme with the increase in β-sheet crystalline content. At pH 7.2, lysozyme (pI 11) and silk (pI 4) [21] were oppositely charged resulting in partitioning between silk films and the buffer. The extent of this partitioning was determined by the changes in secondary structure of the films. This may be attributed to the change in function and/or accessibility of the interaction sites due to formation of β-sheets. The lower permeability of the 6 h W.A. films may have resulted from the strong interaction demonstrated by these films with lysozyme as well as the larger hydrodynamic radius of the compound. An increase in the crystallinity of silk reduced the magnitude of these interactions, which may have promoted mass transport of a larger number of molecules. Therefore, the permeability of the 15 h W.A. and the sequentially treated (15 h W.A. + 2 h M.A) films increased, despite a corresponding reduction in the film hydration. The decrease in the permeability of the 2 h M.A. films for lysozyme may be associated with both lower hydration and stronger partitioning of lysozyme with the films. The permeability of the 6 h W.A. films varied significantly from those subjected to methanol based annealing. The change in the permeability between the two methanol based treatments was not statistically significant. Similar observations were made for the two

treatments based exclusively on water annealing. A lack of observed statistical significance may be a result of the intrinsic variability associated with silk from different preparations.

3.2 Diffusion coefficient

The mass transport characteristics were further studied by calculating the diffusion coefficients of the two model compounds using equation 3. With moderation in the β-sheet content of the films, the diffusion coefficients of vitamin B12 varied from $6.38 \pm 0.37 \times 10^{-6}$ to $0.34 \pm 0.03 \times 10^{-6}$ cm^2 s^{-1} while those of lysozyme varied from $0.113 \pm 0.032 \times 10^{-6}$ to $0.042 \pm 0.018 \times 10^{-6}$ cm^2 s^{-1}. With the exception of 2 h M.A. films, diffusivity of vitamin B12 was at least an order of magnitude greater than that of lysozyme at equivalent β-sheet content (Table 1).

The diffusivity of the compounds was examined in light of the free volume theory described by Yasuda [32]. According to this theory, diffusion of a solute through a polymer matrix is assumed to occur through the free volume present in the matrix. The free volume is described as the fluctuating space within the matrix, not occupied by the polymer chains. This theory relates the diffusivity of the solute to its size and hydration of the film. It can be expressed mathematically by (Eq 5) [25]

$$\ln D = \ln D_0 - Y\,(1/H - 1) \tag{5}$$

Here, D (cm^2 s^{-1}) is the diffusion coefficient of the solute through the polymer, D_0 (cm^2 s^{-1}) is the diffusion coefficient of the solute in water, Y (dimensionless) is a characteristic constant of a solute-solvent combination and H (dimensionless) is the hydration of the film. Compounds obeying the free volume theory are expected to have a linear relationship between ln D and 1/H.

The diffusion of vitamin B12 was consistent with the free volume theory as demonstrated by the high linearity ($R^2 > 0.96$) between the two parameters shown in Figure 4. This confirmed that diffusion of B12 was independent of the compound-matrix interactions and occurred through the solvent filled channels within the film. The diffusivity of lysozyme deviated significantly from the free volume theory. This may be a result of the interaction between the lysozyme and silk that was not accounted for by this theory.

Further mathematical models were investigated to define the relationship between diffusivity of the model compounds and β-sheet crystallinity of the silk films. Only the diffusivity of vitamin B12 could be fitted adequately to a mathematical model. The relationship between diffusivity of vitamin B12 and β-sheet crystallinity was modeled by a power law curve defined in Figure 5. This indicated that the diffusivity of vitamin B12 was more sensitive to small changes in the crystallinity at low β-sheet content. A limiting value of diffusivity may also be postulated at high β-sheet content of the film. However at high β-sheet content, silk exhibited brittle characteristics that may impede measurement of the transport parameters.

4 Conclusions

Controlled mass transfer of two compounds varying in molecular size and ionic character across silk films was achieved by sequentially varying β-sheet crystalline content. The relationship between β-sheet content and diffusivity of vitamin B12 was defined by power law kinetics. The diffusion of vitamin B12 appeared to rely predominantly on the hydration of the films, while that of lysozyme was likely influenced by interactions with silk. Since,

both the silk hydration and the compound-silk interaction were influenced by the β-sheet content of the films, controlling the β-sheet formation could be applied to regulate the mass transport through silk matrices. The results of this study can be useful in the development of coatings for stents or solid drug dosages to obtain predictable release rates as well as to design coatings and delivery systems with longer term sustained release. Moreover this can be achieved under ambient processing conditions that are particularly suited for controlled delivery sensitive drug molecules.

Acknowledgments

The authors thank Dr. Xiaoqin Wang, Dr. Biman Mandal, BalajiKarthick Subramanian, Eleanor Pritchard, Roberto Elia, and Daniel Hines for technical assistance in experiments or writing. This work was supported with financial resources provided by NIH (EB002520) Tissue Engineering Resource Center.

References

1. Kost J, Langer R. Controlled release of bioactive agents. Trends Biotechnol. 1984; 2:47.
2. Ulrich KE, Cannizzaro SM, Langer RS, Shakesheff KM. Polymeric Systems for Controlled Drug Release. Chem Rev. 1999; 99:3181. [PubMed: 11749514]
3. Waeckerle-Men Y, Groettrup M. PLGA microspheres for improved antigen delivery to dendritic cells as cellular vaccines. Adv Drug Deliv Rev. 2005; 57:475. [PubMed: 15560953]
4. Rosen HB, Chang J, Wnek GE, Linhardt RJ, Langer R. Bioerodible polyanhydrides for controlled drug delivery. Biomaterials. 1983; 4:131. [PubMed: 6860755]
5. Fu K, Pack DW, Klibanov AM, Langer R. Visual evidence of acidic environment within degrading poly(lactic-co-glycolic acid) (PLGA) microspheres. Pharmaceutical Research. 2000; 17:100. [PubMed: 10714616]
6. Zignani M, Bernatchez SF, Le Minh T, Tabatabay C, Anderson JM, Gurny R. Subconjunctival biocompatibility of a viscous bioerodable poly(ortho ester). J Biomed Mater Res. 1998; 39:277. [PubMed: 9457558]
7. Poshusta AK, Burdick JA, Mortisen DJ, Padera RF, Ruehlman D, Yaszemski MJ, et al. Histocompatibility of photocrosslinked polyanhydrides: A novel in situ forming orthopaedic biomaterial. Journal of Biomedical Materials Research Part A. 2003; 64A:62. [PubMed: 12483697]
8. Agnihotri SA, Mallikarjuna NN, Aminabhavi TM. Recent advances on chitosan-based micro- and nanoparticles in drug delivery. J Controlled Release. 2004; 100:5.
9. Friess W. Collagen – biomaterial for drug delivery. European Journal of Pharmaceutics and Biopharmaceutics. 1998; 45:113. [PubMed: 9704909]
10. Heras A, Rodríguez NM, Ramos VM, Agulló E. N-methylene phosphonic chitosan: a novel soluble derivative. Carbohydr Polym. 2001; 44:1.
11. Sofia S, McCarthy MB, Gronowicz G, Kaplan DL. Functionalized silk-based biomaterials for bone formation. J Biomed Mater Res. 2001; 54:139. [PubMed: 11077413]
12. Meinel L, Hofmann S, Karageorgiou V, Kirker-Head C, McCool J, Gronowicz G, et al. The inflammatory responses to silk films in vitro and in vivo. Biomaterials. 2005; 26:147. [PubMed: 15207461]
13. Tang X, Ding F, Yang Y, Hu N, Wu H, Gu X. Evaluation on in vitro biocompatibility of silk fibroin-based biomaterials with primarily cultured hippocampal neurons. J Biomed Mater Res. 2009; 91A:166.
14. Wang Y, Rudym DD, Walsh A, Abrahamsen L, Kim H, Kim HS, et al. In vivo degradation of three-dimensional silk fibroin scaffolds. Biomaterials. 2008; 29:3415. [PubMed: 18502501]
15. Horan RL, Antle K, Collette AL, Wang Y, Huang J, Moreau JE, et al. In vitro degradation of silk fibroin. Biomaterials. 2005; 26:3385. [PubMed: 15621227]
16. Lu Q, Wang X, Hu X, Cebe P, Omenetto F, Kaplan DL. Stabilization and release of enzymes from silk films. Macromolecular Bioscience. 2010; 10:359. [PubMed: 20217856]
17. Wenk E, Wandrey AJ, Merkle HP, Meinel L. Silk fibroin spheres as a platform for controlled drug delivery. J Controlled Release. 2008; 132:26.

18. Wang X, Kluge JA, Leisk GG, Kaplan DL. Sonication-induced gelation of silk fibroin for cell encapsulation. Biomaterials. 2008; 29:1054. [PubMed: 18031805]
19. Bayraktar O, Malay Ö, Özgarip Y, Batıgün A. Silk fibroin as a novel coating material for controlled release of theophylline. European Journal of Pharmaceutics and Biopharmaceutics. 2005; 60:373. [PubMed: 15996578]
20. Hofmann S, Wong Po Foo CT, Rossetti F, Textor M, Vunjak-Novakovic G, Kaplan DL, et al. Silk fibroin as an organic polymer for controlled drug delivery. J Controlled Release. 2006; 111:219.
21. Wang X, Hu X, Daley A, Rabotyagova O, Cebe P, Kaplan DL. Nanolayer biomaterial coatings of silk fibroin for controlled release. J Controlled Release. 2007; 121:190.
22. Wilz A, Pritchard EM, Li T, Lan J, Kaplan DL, Boison D. Silk polymer-based adenosine release: Therapeutic potential for epilepsy. Biomaterials. 2008; 29:3609. [PubMed: 18514814]
23. Li C, Vepari C, Jin H, Kim HJ, Kaplan DL. Electrospun silk-BMP-2 scaffolds for bone tissue engineering. Biomaterials. 2006; 27:3115. [PubMed: 16458961]
24. Lawrence B, Omenetto F, Chui K, Kaplan D. Processing methods to control silk fibroin film biomaterial features. J Mater Sci. 2008; 43:6967.
25. Sung KC, Topp EM. Effect of drug hydrophilicity and membrane hydration on diffusion in hyaluronic acid ester membranes. J Controlled Release. 1995; 37:95.
26. Wang X, Wenk E, Matsumoto A, Meinel L, Li C, Kaplan DL. Silk microspheres for encapsulation and controlled release. J Controlled Release. 2007; 117:360.
27. Hu X, Kaplan D, Cebe P. Determining beta-sheet crystallinity in fibrous proteins by thermal analysis and infrared spectroscopy. Macromolecules. 2006; 39:6161.
28. Byun Y, Jeong S, Kim Y. Mechanism of urea effect on percutaneous absorption of clonidine. Archives of Pharmacal Research. 1989; 12:143.
29. Wang X, Yucel T, Lu Q, Hu X, Kaplan DL. Silk nanospheres and microspheres from silk/pva blend films for drug delivery. Biomaterials. 2010; 31:1025. [PubMed: 19945157]
30. Lu Q, Hu X, Wang X, Kluge JA, Lu S, Cebe P, et al. Water-insoluble silk films with silk I structure. Acta Biomaterialia. 2010; 6:1380. [PubMed: 19874919]
31. Jin HJ, Park J, Karageorgiou V, Kim UJ, Valluzzi R, Cebe P, et al. Water-Stable Silk Films with Reduced β-Sheet Content. Advanced Functional Materials. 2005; 15:1241.
32. Yasuda H, Lamaze CE, Ikenberry LD. Permeability of solutes through hydrated polymer membranes. Part I. Diffusion of sodium chloride. Die Makromolekulare Chemie. 1968; 118:19.
33. Bell CL, Peppas NA. Water, solute and protein diffusion in physiologically responsive hydrogels of poly (methacrylic acid-g-ethylene glycol). Biomaterials. 1996; 17:1203. [PubMed: 8799505]

Highlights

- Effect of silk β-sheet crystallinity on transport of model compounds is studied.
- Crystalline content relates to vitamin B12 diffusivity through a power law model.
- Lysozyme-silk interactions result in non-compliance with free volume theory.
- We underscore potential of silk for controlled delivery of therapeutic agents.

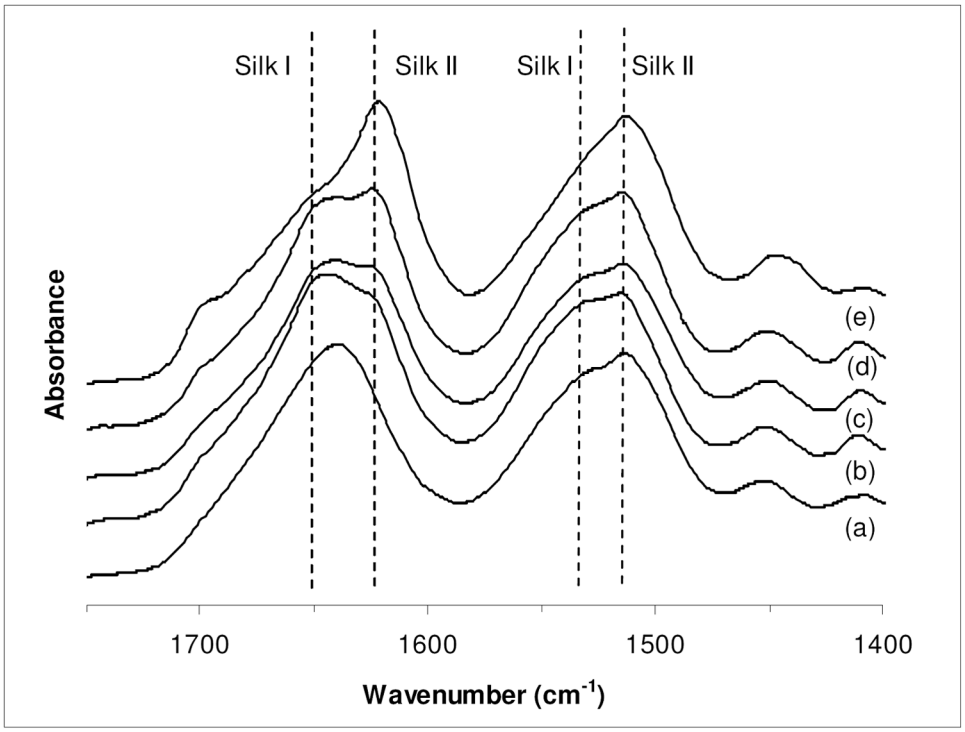

Figure 1.

Absorbance spectra of silk films: (a) cast silk film (b) 6 h water annealed silk film; (c) 15 h water annealed silk film (d) 15 h water annealed plus 2 h methanol annealed film; (e) 2 h methanol annealed film, characterized by FTIR spectroscopy in the amide I (1700 cm^{-1} to 1600 cm^{-1}) and amide II (1600 cm^{-1} to 1500 cm^{-1}) region.

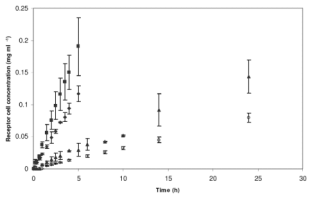

Figure 2.
Receptor cell concentration of vitamin B12 diffusing through: (◆) 6 h water annealed, (■) 15 h water annealed, (▲) 15 h water annealed followed by 2 h methanol annealed and (○) 2 h methanol annealed silk films.

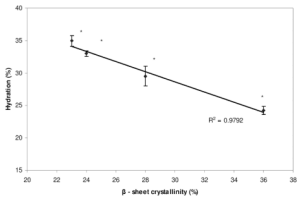

Figure 3.
Effect of annealing treatments (β-sheet crystallinity) on the hydration of silk films. (*Data statistically significant ($p < 0.05$), $n = 5$)

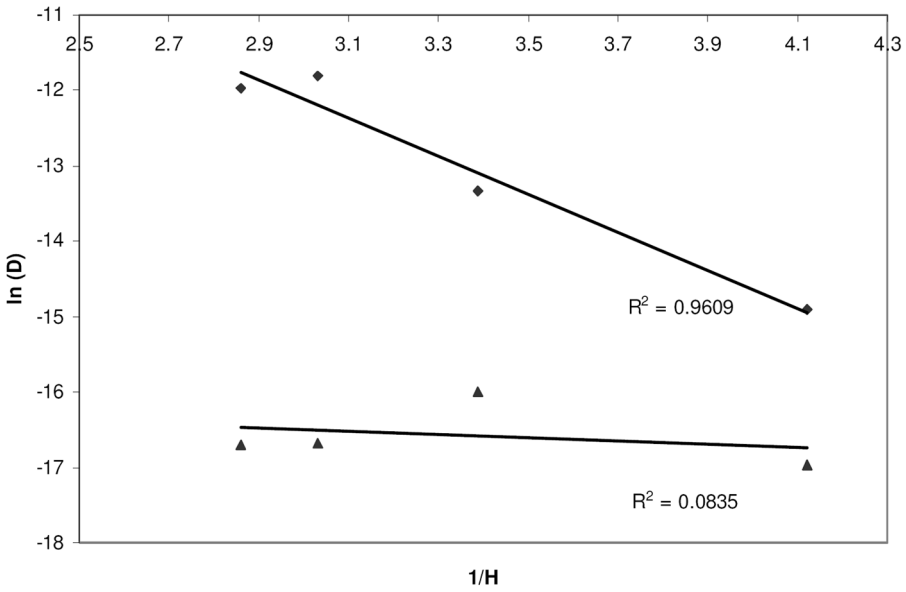

Figure 4.
Natural logarithm of diffusion coefficients of (◆) vitamin B12 and (▲) FITC-lysozyme plotted as a function of reciprocal of film hydration to test for the free volume theory. Linearity indicates agreement with theory.

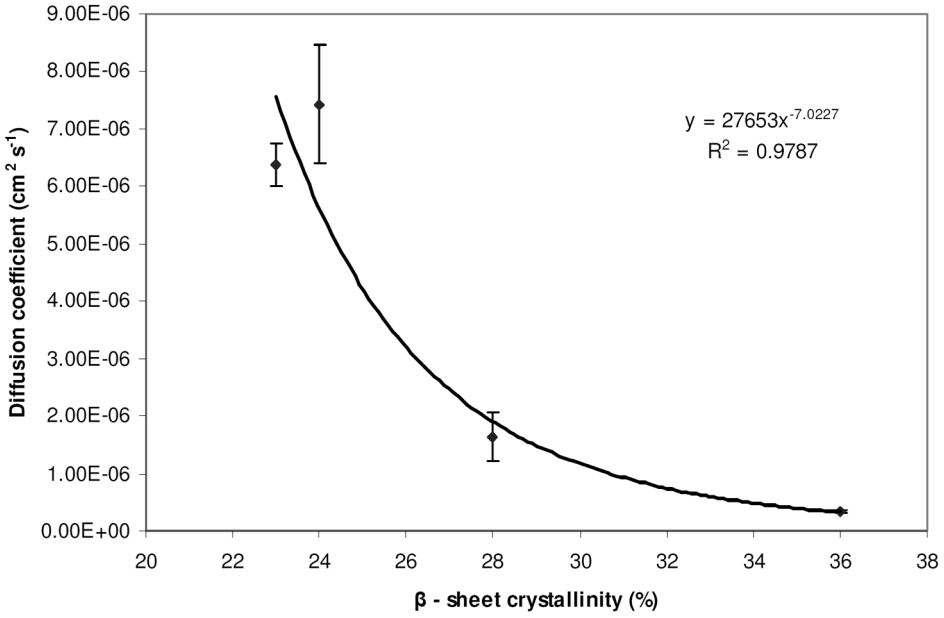

Figure 5.
Power law model fitted to characterize change in diffusion coefficients of vitamin B12 as a function of β-sheet crystallinity.

Table 1

Model compounds used in mass transport studies [34].

Compound	Molecular weight (kDa)	Hydrodynamic radius (nm)	Iso-electric point
Vitamin B12	1.34	0.85	--
Lysozyme	14.1	1.60	11

Table 2

Partition, permeability and diffusion coefficients of vitamin B12 and lysozyme as a function of β-sheet crystallinity of silk films.

Treatment	β Sheet (%)	Compound	Partition Coefficient (K_d)	Permeability Coefficient (cm/s) ($\times 10^{-1}$)	Diffusion Coefficient (D) (cm^2/s) ($\times 10^{-6}$)
6 h W.A.	23	B12	4.76 ± 1.77	1.08 ± 0.064*	6.38 ± 0.37*
15 h W.A.	24		5.35 ± 1.42	1.55 ± 0.213*	7.34 ± 1.02†
15 h W.A. + 2 h M.A.	28		6.45 ± 0.39	0.41 ± 0.104*	1.64 ± 0.28*†‡
2 h M.A.	36		12.51 ± 1.04*	0.16 ± 0.017*	0.34 ± 0.03*†‡
6 h W.A.	23	Lysozyme	72.91 ± 4.55*†	0.029 ± 0.003$^{\dagger *}$	0.056 ± 0.011*
15 h W.A.	24		29.23 ± 5.24*	0.059 ± 0.022	0.057 ± 0.021
15 h W.A. + 2 h MA.	28		21.48 ± 4.88†‡	0.086 ± 0.025†	0.113 ± 0.032*†
2 h M.A.	36		51.14 ± 13.40‡	0.077 ± 0.033*	0.042 ± 0.018†

‡, †, *Data statistically significant ($p < 0.05$), n=3

W.A. – Water annealed, M.A. – Methanol annealed

J Memb Sci. Author manuscript; available in PMC 2012 November 1.